

Efflux only impacts drug accumulation in actively growing cells

Emily E Whittle¹, Helen E McNeil¹, Eleftheria Trampari², Mark Webber², Tim W Overton³, Jessica M A Blair^{1*}

¹College of Medical and Dental Sciences, Institute of Microbiology and Infection, University of Birmingham, Birmingham, UK

²Quadrant Institute Bioscience, Norwich Research Park, Norwich, United Kingdom

³School of Chemical Engineering, University of Birmingham, Birmingham, UK.

***Correspondence:**

Jessica M A Blair

J.M.A.Blair@bham.ac.uk

Abstract

For antibiotics with intracellular targets, effective treatment of bacterial infections requires the drug to accumulate to a high concentration inside cells. Bacteria produce a complex cell envelope and possess drug-export efflux pumps to limit drug accumulation inside cells. Decreasing cell envelope permeability and increasing efflux pump activity can reduce intracellular accumulation of antibiotics, and are commonly seen in antibiotic resistant strains. Here, we show that the balance between influx and efflux differs depending on bacterial growth phase in Gram-negative bacteria. Accumulation of the model fluorescent drug, ethidium bromide (EtBr) was measured in *S. Typhimurium* SL1344 (wild-type) and efflux deficient ($\Delta acrB$) strains during growth. In SL1344, EtBr accumulation remained low,

regardless of growth phase and did not correlate with *acrAB* transcription. EtBr accumulation in $\Delta acrB$ was high in exponential phase but dropped sharply later in growth, with no significant difference to SL1344 in stationary phase. Low EtBr accumulation in stationary phase was not due to the upregulation of other efflux pumps, but instead, due to decreased permeability of the envelope in stationary phase. RNAseq identified changes in expression of several pathways that remodel the envelope in stationary phase, leading to lower permeability. This study shows that efflux is only important for maintaining low drug accumulation in actively growing cells, and that envelope permeability is the predominant factor dictating the rate of drug entry in stationary phase cells. This conclusion means that (i) antibiotics with intracellular targets may be less effective in complex non-growing or slow-growing bacterial infections where intracellular accumulation may be low, (ii) efflux inhibitors may be successful in potentiating the activity of existing antibiotics, but potentially only for bacterial infections where cells are actively growing and (iii) the remodelling of the cell envelope prior to stationary phase could provide novel drug targets.

1 **Introduction**

2 Antibiotic treatment failure in clinical infections is increasingly common due to the
3 rise in multi-drug resistant (MDR) Gram-negative bacteria. Gram-negative infections
4 are particularly difficult to treat due to their impermeable outer membranes and efflux
5 pumps which actively export antibiotic molecules out of the bacterial cell. Successful
6 treatment relies on high concentrations of antibiotic accumulating within bacterial
7 cells, which is a function of antibiotic influx and the rate of antibiotic efflux¹.

8 Small hydrophilic antibiotics such as β -lactams enter a Gram-negative bacterial cell
9 through membrane pores called porins. The major porins of *Enterobacteriaceae* are
10 OmpF and OmpC². Downregulation of porin genes contributes to antibiotic
11 resistance by preventing antibiotics entering the cell³. In addition, mutations in the
12 porin protein which change the channel diameter^{4,5} or the electric field inside the
13 porin can block translocation of drugs across the membrane⁵.

14 Some drugs can enter Gram-negative cells through the lipid outer and inner
15 membranes via 'self-promoted uptake'. This mechanism has been described for
16 EDTA, Polymyxin B, colistin and other cationic antimicrobial peptides (CAMPs), and
17 aminoglycoside antibiotics⁶⁻⁸. The chelator, EDTA, acts as a permeabiliser by
18 displacing and chelating the cations (Mg^{2+} or Ca^{2+}) that are essential for the stability
19 of LPS and the OM^{6,9}. CAMPs interact with anionic groups on lipid A, breaching the
20 outer membrane, and porate in the inner membrane, leading to bacterial death.

21 *Enterobacteriaceae* contain efflux pumps from 6 classes. MFS, SMR, MATE, RND
22 and the recently described PACE pumps¹⁰ utilise the proton motive force for export
23 of molecules such as antibiotics, and ABC (ATP binding cassette) pumps utilise ATP

24 hydrolysis. Resistance-Nodulation-Division (RND) pumps are commonly upregulated
25 in clinical isolates and can contribute to resistance to a number of antibiotic classes,
26 as well as dyes, detergents and biocides¹¹. The best described RND pump is AcrAB-
27 TolC, found in *Salmonella enterica* serovar Typhimurium (S. Typhimurium) and *E.*
28 *coli*. As efflux pumps underpin antibiotic resistance in essentially all bacteria of
29 clinical and veterinary importance^{12,13} there is ongoing active research into the
30 development of efflux inhibitors to potentiate the action of existing antibiotics.

31 Previous studies undertaken with cells in exponential growth phase have highlighted
32 the importance of efflux pumps in minimising intracellular drug accumulation¹⁴⁻¹⁷.
33 However, transcription of *acrAB* is growth phase dependent, with a peak in mid-
34 exponential phase, which drops as cells enter into stationary phase¹⁸. The
35 importance of AcrAB-TolC in bacterial cells in stationary phase which are slow-
36 growing or non-growing is not known. However, it has been suggested that whereas
37 survival of exponential-phase *E. coli* following treatment with the anionic detergent
38 sodium dodecyl sulphate (SDS) is dependent on efflux, stationary phase cell survival
39 is efflux-independent and rather is mediated by decreased permeability of the
40 bacterial cell envelope, directed by the stationary phase sigma factor RpoS¹⁹. Little is
41 known about the balance between influx and efflux in different growth phases and
42 how this may relate to different growth states that may occur in an infection.

43 Previous studies have shown that the *E. coli* envelope changes in stationary phase
44 when compared to logarithmic growth and it is possible that this could alter antibiotic
45 influx in non-growing bacterial cells. Outer membrane changes include a decrease in
46 the overall concentration of membrane proteins²⁰ and an increase in lipoprotein
47 crosslinked to peptidoglycan^{21,22} to strengthen the outer barrier. In the inner

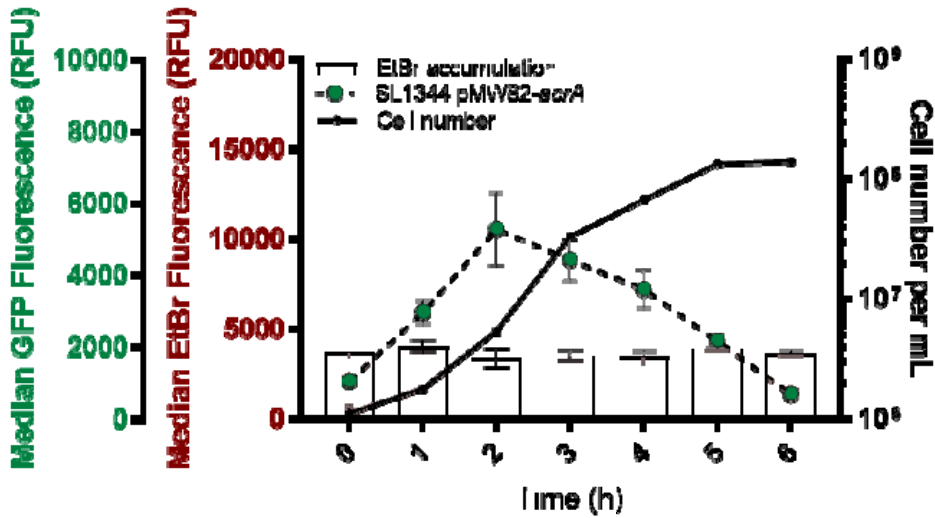
48 membrane, the composition of fatty acids changes with a decrease in
49 monounsaturated fatty acids²³ and an increase in cyclopropane fatty acids, catalysed
50 by Cfa²⁴. Increased layers of peptidoglycan have also been described in stationary
51 phase²⁵.

52 Using a combination of fluorescent drug accumulation assays¹⁷, and measurement
53 of efflux gene transcription in wild-type and efflux mutant strains we here assess the
54 importance of the balance between influx and efflux in different growth phases in
55 Gram-negative bacteria, using the model organism *Salmonella enterica* serovar
56 Typhimurium. We also use RNASeq to measure the global transcriptome as bacteria
57 enter stationary phase and correlate transcriptomic changes with biochemical and
58 physiological changes in the cell envelope that lead to alterations in permeability.

59 **Results**

60 **Accumulation level of drugs by *S. Typhimurium* is independent of growth
61 phase-dependent *acrAB* transcription**

62 Using a recently developed flow cytometry method¹⁷, both the intracellular
63 accumulation of the fluorescent dye ethidium bromide (EtBr), and the transcription of
64 *acrAB* (via a promoter-GFP fusion) were measured in parallel in single cells of
65 *Salmonella* grown in *drug free* media. Samples were taken hourly during batch
66 culture before EtBr was added to the sample immediately prior to flow cytometry
67 analysis to measure accumulation (EtBr was *not* present in growing the culture).



68

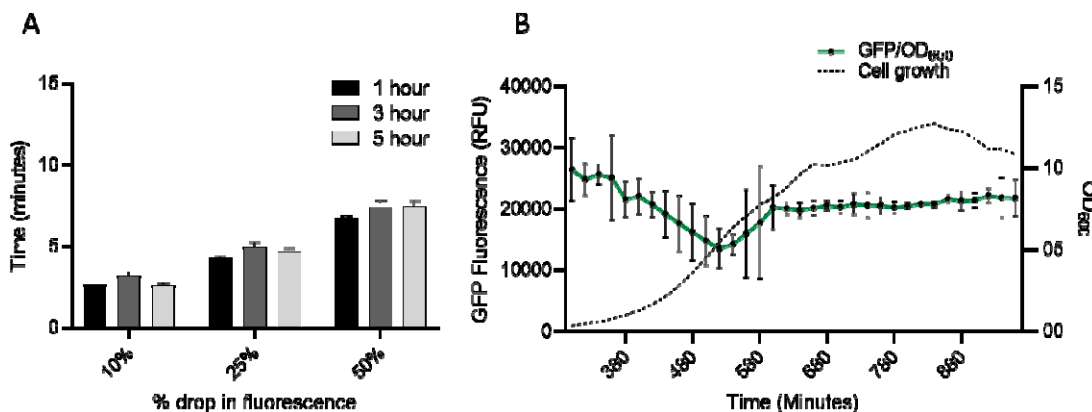
69 **Figure 1 Ethidium bromide accumulation and *acrAB* expression in single cells of *S. Typhimurium* SL1344**
70 **across the growth phase.** Cell number per mL was measured in each sample (black lines, numbers indicated
71 on the right y-axis). Pink bars indicate median ethidium bromide fluorescence per cell (relating to left red y-axis)
72 and dashed lines with green circles show *acrAB* expression (median GFP fluorescence per cell from reporter,
73 relating to left green y-axis. All data points are median values from measurements of 10,000 single cells of
74 SL1344. Error bars indicate standard error of the mean (+/- SEM).

75 Transcription of *acrAB* in SL1344 was growth phase dependent and peaked in early-
76 mid log phase before decreasing towards stationary phase (**Figure 1**), as previously
77 described¹⁸. Previous studies have shown that increased expression of *acrAB* in
78 clinical isolates leads to decreased susceptibility to antibiotics¹². Given the known
79 role of efflux pumps in drug export, one might predict that EtBr accumulation would
80 be lowest when efflux expression was highest. Our data however show that this is
81 not the case. In SL1344 cells, accumulation of EtBr was low and remained
82 unchanged across growth despite changes in *acrAB* transcription (Fig 1). Therefore,
83 changes in efflux pump transcription in different growth phases does not alter levels
84 of drug accumulation within the cell.

85 **Growth phase-dependent transcription of *acrAB* does not correlate with drug**
86 **accumulation, efflux capacity or AcrAB protein level**

87 Having shown that *acrAB* transcription does not correlate with ethidium bromide
88 accumulation, the efflux function in a population of cells was measured to determine
89 whether efflux activity varied with growth phase (and *acrAB* expression), even if drug
90 accumulation did not.

91 To measure functional efflux capacity of cells we used the previously described
92 direct efflux activity assay¹⁴ which was further optimised to analyse efflux capacity at
93 3 different time points across growth in SL1344. This assay determines the efflux
94 capacity of the cell based on the activity of all efflux pumps (not just AcrAB-TolC)
95 that are able to transport EtBr. Cultures grown for 1, 3 and 5 hours had the same
96 capacity to efflux the substrate as there was no significant difference in efflux rate
97 between samples taken at each time point (**Figure 2A**) (based on time taken for
98 ethidium bromide fluorescence to drop 10%, 25% and 50% from its maximum
99 fluorescence value) regardless of the different levels of *acrAB* transcription at these
100 time points already established.



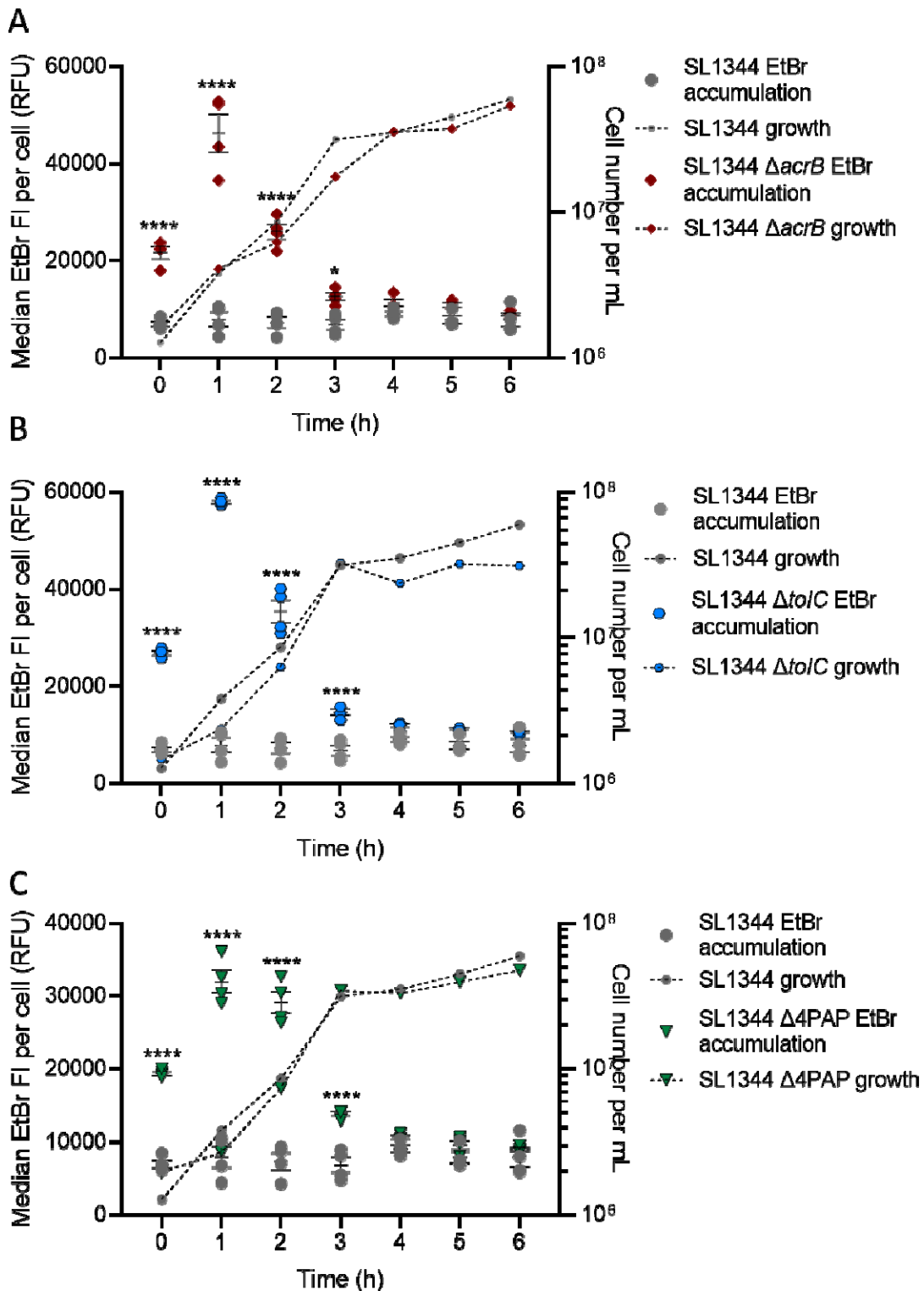
101
102 **Figure 2 (A)** Time taken for ethidium bromide to be removed from SL1344 cells at 1,3 and 5 hours. Bars
103 represent the time taken for ethidium bromide fluorescence to drop 10%, 25% and 50% from its original value.
104 Data is based on 3 biological replicates with error bars showing standard error of the means (SEM). 1 hour
105 (black), 3 hours (dark grey) and 5 hours (light grey) are shown. There was no significant difference in the time
106 taken to export EtBr at each time point. **(B)** GFP/OD₆₀₀ from SL1344 AcrB-GFP over 16 hours of growth in
107 MOPs minimal media. This graph shows GFP/OD₆₀₀ from AcrB-GFP at the end of lag phase (300 minutes) until
108 the last time point at 16 hours. The dashed black line shows the OD₆₀₀ whereas the green line error bars +/- SEM
109 shows GFP fluorescence. SL1344 autofluorescence was subtracted from this data.

110 Taken together, the low accumulation and similar rate of efflux of EtBr across time in
111 SL1344 suggests that although *acrAB* transcription peaks in mid-exponential phase,
112 activity of the assembled AcrAB-TolC complex remains constant. The AcrB protein is
113 known to be very stable once made with a predicted half-life of 6 days²⁶. To measure
114 AcrB protein level at different points during growth a strain was constructed in which
115 the AcrB protein was tagged with GFP at the C-terminus as previously described²⁷.
116 The generation time and efflux level in this strain were unaffected confirming that
117 tagging GFP to the C-terminus of AcrB did not affect its function. Measurement of
118 GFP fluorescence during 16 hours of growth showed that AcrB level remains
119 constant (**Figure 2B**). These data suggest that efflux capacity is constant regardless
120 of growth phase due to the constant level of AcrAB protein within a population and
121 may explain why EtBr accumulation remained low in stationary phase despite
122 decreased efflux gene transcription.

123 **Drug accumulation is only dependent on efflux in actively growing cells**

124 To further dissect the importance of efflux during different growth stages we
125 measured EtBr accumulation (as in Fig. 1) in the presence or absence of AcrAB-
126 TolC function (using SL1344 $\Delta acrB$). The previous results suggest AcrAB-TolC
127 activity is constant, therefore by removing the efflux pump, it was assumed that EtBr
128 accumulation would be high across growth. When measuring EtBr accumulation in
129 SL1344 $\Delta acrB$, after 1 hour of growth, EtBr accumulation was 6-fold higher than in
130 SL1344. This is similar to the growth time point used in most other published studies
131 that have shown an increase in accumulation upon deletion of *acrB*^{11,14,15,17}.
132 However, EtBr accumulation then decreased dramatically and was not significantly
133 different from WT from 3-6 hours of growth (**Figure 3A**). This suggests that low

134 accumulation at 1 hour in SL1344 greatly depends on efflux to export ethidium
135 bromide from actively growing cells. As there is no significant difference between
136 $\Delta acrB$ and WT cells from 3-6 hours, it suggests that AcrAB-TolC is not important in
137 maintaining low accumulation in slower growing or stationary phase cells. This is
138 also supported by the *acrAB* expression data which shows highest expression in the
139 early stages of logarithmic growth.



140

141 **Figure 3 EtBr accumulation in SL1344 and SL1344 Δ acrB (A), Δ toIC (B) and Δ 4PAP (C).** For each strain the
142 median EtBr fluorescence per cell in 10,000 single cells was measured every hour between 0 and 6 hours of
143 growth for SL1344 (Grey circles) and (A) SL1344 Δ acrB (red diamonds) (B) Δ toIC (blue hexagons) and (C)
144 Δ 4PAP (Δ acrA Δ acrB Δ mdtA Δ mdtB) (green triangles). Data from 4 biological replicates for each strain are
145 shown, horizontal bars show the mean and error bars the SEM. Median EtBr fluorescence per cell is plotted on

146 the left y-axis. Calculated cell number per mL values were plotted on the right y-axis with corresponding symbols
147 equating to strain and a dashed line to show growth of the cultures. Cell numbers were based on the mean of the
148 same biological replicates and the same gated population that EtBr fluorescence was measured from. Two-way
149 ANOVA and Sidak's multiple comparison test were carried out for statistical analysis. At 0, 1 and 2 hours, EtBr
150 accumulation was significantly increased in $\Delta acrB$ with p values of <0.0001 (****). At 0, 1, 2 and 3 hours, EtBr
151 accumulation was significantly increased in $\Delta tolC$ and $\Delta 4PAP$ with p values of <0.0001.

152 To confirm that low EtBr accumulation in stationary phase was not due to the activity
153 of other RND efflux pumps present in SL1344, EtBr accumulation was also
154 measured in two other mutants of SL1344. In the first, *tolC* was deleted which
155 compromises most efflux systems in *Salmonella* which use TolC as a common outer
156 membrane channel. The second strain used lacked all four periplasmic adaptor
157 proteins ($\Delta 4PAP$; $\Delta acrA$ $\Delta acrE$ $\Delta mdsA$ $\Delta mdtA$) and is incapable of assembling any
158 functional RND efflux systems. In both strains, the EtBr accumulation pattern
159 observed recapitulated that seen in SL1344 $\Delta acrB$, with a peak in accumulation at 1
160 hour, but no significant difference to SL1344 in stationary phase cells (**Figure 3B&C**). This result showed that low accumulation in stationary phase was not due to
161 any RND pump in SL1344, (nor the ABC pump MacAB-TolC). In addition, we also
162 showed that, apart from *acrAB* whose transcription was highest in mid-log phase and
163 lowest in stationary phase, no other RND pump was actively transcribed in the
164 conditions used to measure accumulation capacity across growth (**Figure S1**). For
165 pumps from other families, only *macA* (ABC), *mdtA* (MFS) and *mdtK* (MATE) were
166 transcribed and only at low levels (**Figure S1**).

168 Further investigation into the role of efflux pumps in stationary phase EtBr
169 accumulation was carried out by measurement in the presence of the proton motive
170 force inhibitor CCCP. Inhibiting the proton motive force, inhibits the activity of the
171 RND, MFS and MATE pumps of SL1344^{28,29}. In SL1344 in the presence of CCCP,
172 EtBr accumulation peaked at 1 hour (**Figure S2**). Accumulation levels started to drop
173 into stationary phase, strikingly similar to SL1344 $\Delta acrB$, again suggesting that low

174 accumulation in stationary phase is not dependent on RND, MFS or MATE-mediated
175 efflux. This independent confirmation using different mutants and inhibitors
176 demonstrates that the observed low EtBr accumulation in stationary phase is efflux-
177 independent.

178 To investigate whether this was just a *Salmonella* phenomenon, EtBr accumulation
179 was measured in wild-type and a mutant lacking major RND efflux pump of other
180 Gram-negative bacterial species including *Escherichia coli* (MG1655 and MG1655
181 $\Delta acrB$), *Pseudomonas aeruginosa* (PA01 and PA01 $\Delta mexA$) and *Klebsiella*
182 *pneumoniae* (ecl8 and ecl8 $acrB::Gm$). In *E. coli* and *K. pneumoniae*, EtBr
183 accumulation was low throughout growth for the wild-type but peaked at 1 hour for
184 each *acrB* mutant (**Figure S3**) and in *P. aeruginosa*, the *mexA* mutant peaked at 2
185 hours (**Figure S4**) and then dropped to WT levels in stationary phase. Therefore,
186 very similar observations are seen in a wide range of Gram-negative organisms.

187 The EtBr accumulation pattern in *Salmonella* was also shown in MOPS minimal
188 medium suggesting that the pattern was not influenced by media type and
189 specifically was not a result of the limitations of LB³⁰ (**Figure S5**). Even though is a
190 well-established and studied model efflux substrate, to counter the possibility that
191 EtBr would give abnormal results which are not representative of other efflux
192 substrates, the same accumulation pattern in *Salmonella* WT and $\Delta tolC$ was also
193 shown using the lipophilic dye Nile Red (**Figure S6**). Unlike EtBr, Nile Red does not
194 fluoresce on intercalation with DNA, but rather when bound to phospholipids or
195 triglycerides³¹ showing this is not an artefact of the dye initially used. Together this
196 data shows that the accumulation pattern described in the absence of efflux is
197 consistent regardless of Gram-negative species, media type or efflux substrate used.

198 **Drug accumulation in stationary phase is controlled by reduced membrane**

199 **permeability**

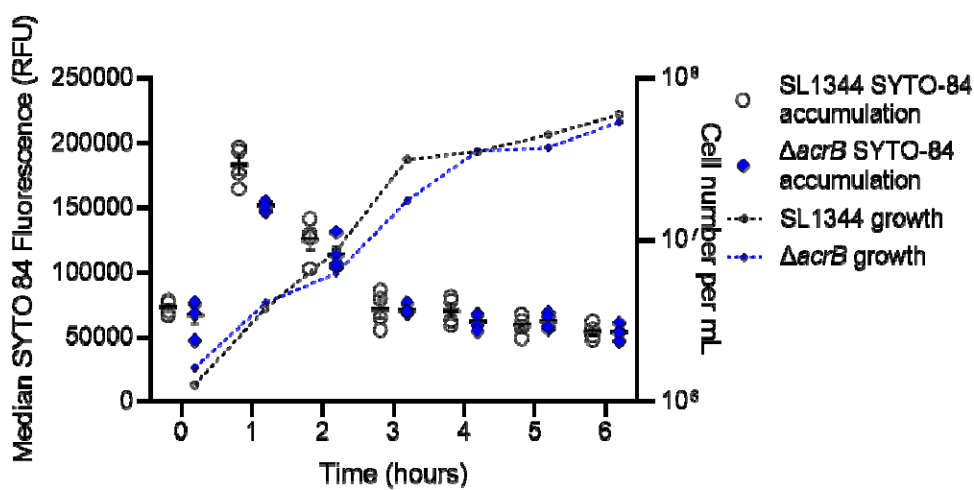
200 Together this data shows that cells from later growth phases minimise intracellular
201 accumulation of EtBr (and other substrates) in an efflux independent manner. We
202 hypothesised this could be due to a shift in the balance between influx and efflux
203 over growth, with influx rate, controlled by reduced permeability of the outer
204 membrane, being more important in slower growing or stationary phase cells.

205 Several dyes that are often used to probe the permeability of the outer membrane,
206 such as NPN (1-N-Phenylnaphthylamine), are efflux substrates and therefore
207 assessing membrane permeability in strains lacking efflux pumps is problematic.

208 Most hydrophilic antibiotics enter Gram-negative bacterial cells through outer
209 membrane porins such as OmpC and OmpF. To investigate whether porins altered
210 the accumulation of EtBr, accumulation assays were performed using SL1344
211 mutants; Δ ompC/ Δ ompF/ Δ acrB, Δ ompC/ Δ acrB, Δ ompF/ Δ acrB, Δ ompC, and Δ ompF
212 and showed that none had a significantly different EtBr accumulation pattern to those
213 previously seen, confirming that EtBr doesn't enter *S. Typhimurium* through OmpF or
214 OmpC (**Figure S7**). A similar observation was made by Murata *et al.* in *E. coli* K-12
215³², who concluded that the OM bilayer is the predominant mode of EtBr entry.

216 Since SYTO 84 is used in our flow cytometry assay as a probe to stain cells, the
217 accumulation of this dye was first investigated to assess permeability and to
218 determine if it is an efflux substrate. SYTO 84 is marketed as a cell-permeant DNA
219 dye and so is expected to readily enter bacteria. There was no significant difference
220 between the accumulation of SYTO 84 in SL1344 and SL1344 Δ acrB and in both
221 strains accumulation peaked after 1 hour of growth (**Figure 4**). This shows that

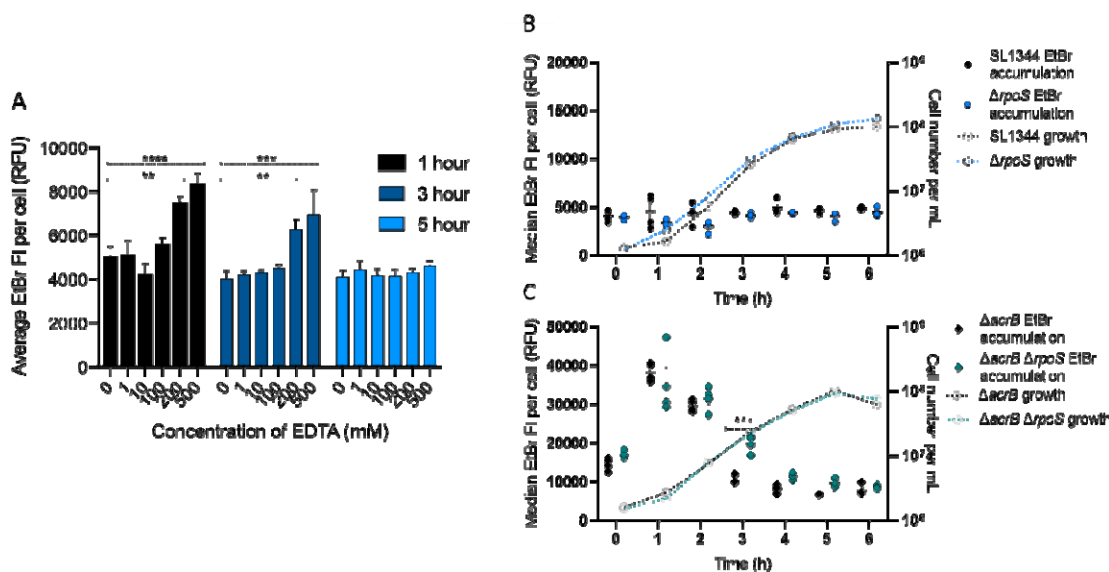
222 SYTO 84 is not an efflux substrate and demonstrates the importance of efflux in
223 maintaining low accumulation of drugs and dyes that are substrates in actively
224 growing cells. However, SYTO 84 fluorescence decreased significantly in both
225 strains on entrance to stationary phase. This suggests that a compound that is not
226 exported via efflux, is also less able to enter bacteria during stationary phase and we
227 hypothesise this is due to a strengthening of the permeability barrier. It is important
228 to note that, although the SYTO 84 fluorescence does reduce around 2.5-fold in
229 stationary phase, the lowest value is still over 45,000 RFU, so the reduction does not
230 compromise its use to differentiate cells from acellular particles in the EtBr
231 accumulation assays using flow cytometry.



232
233 **Figure 4 SYTO 84 accumulation in SL1344 and SL1344 Δ acrB.** Median SYTO 84 fluorescence per cell in
234 10,000 cells was measured every hour between 0 and 6 hours. White circles (SL1344) and blue diamonds
235 (Δ acrB) represent the X-median value of SYTO 84 fluorescence in 10,000 cells within a biological replicate. 4
236 biological replicates for each strain are shown, with +/- SEM error bars. Median SYTO 84 fluorescence is plotted
237 on the left Y-axis. Calculated cell number per mL values were plotted on the right Y-axis with corresponding
238 symbols equating to strain and a dashed line to show growth of the culture. Cell numbers were based on the
239 mean of the same biological replicates and the same gated population that EtBr fluorescence was measured
240 from.

241 Ethidium bromide is a cationic dye that diffuses into cells through the OM³². LPS
242 molecules on the outer face of the outer membrane are ionically cross-linked to each
243 other by divalent cations (Mg^{2+} or Ca^{2+}) binding to phosphate groups in lipid A,

244 generating a permeability barrier. EDTA is considered a 'permeabiliser' which can
245 chelate and thus displace divalent cations, destabilising and releasing LPS³³,
246 thereby increasing the permeability of the cell to itself and other compounds⁶.
247 Increasing concentrations of EDTA were used to permeabilise the outer membrane
248 and assess the effect on ethidium bromide accumulation (**Figure 5A**). Following 1 or
249 3 hours of growth, there was no significant difference in EtBr accumulation up to 100
250 μ M EDTA. At 200 μ M and 500 μ M EDTA, EtBr accumulation was significantly higher,
251 suggesting that EDTA was able to make the outer membrane more permeable to
252 EtBr. At 5 hours, neither 200 μ M nor 500 μ M EDTA had any effect on the
253 accumulation of EtBr. This suggests that the *Salmonella* outer membrane is
254 remodelled during entry into stationary phase and becomes less reliant on cation-
255 mediated crosslinking to maintain its permeability barrier to EtBr. Indeed, both
256 *Salmonella* and *E. coli* become more resistant to CAMPs, whose mode of action
257 relies upon interaction with negative charges on the LPS, in stationary phase^{34,35}



258

259 **Figure 5 (A) EtBr accumulation in SL1344 treated with EDTA.** Bars represent median EtBr fluorescence in
260 10,000 single cells of SL1344. EtBr accumulation was measured in the presence of increasing concentrations of
261 EDTA (0, 1, 10, 100, 200 and 500 mM) from a culture grown for 1 hour (black), 3 hours (dark blue) and 5 hours

262 (light blue). Error bars show SEM from 3 biological replicates. Dashed lines above the bars with asterisks
263 represent significance value when based on a T-test compared to no EDTA added. At 1 hour, treatment with 200
264 and 500 mM significantly increased EtBr accumulation in SL1344 with p values of 0.0013 (**) and <0.0001 (****)
265 respectively. At 3 hours, treatment with 200 and 500 mM significantly increased EtBr accumulation in SL1344
266 with p values of 0.0033 (**) and 0.0001 (**) respectively. **(B+C) EtBr accumulation in SL1344 ΔrpoS and**
267 **ΔacrB ΔrpoS.** 4 biological replicates for each strain are shown, with a short mean bar and SEM error bars. EtBr
268 accumulation is plotted on the left Y-axis. Calculated cell number values were plotted on right Y-axis. Cell
269 numbers were based on the mean of the same biological replicates and the same gated population that EtBr
270 fluorescence was measured from. **(B)** shows SL1344 WT (individual black dots) vs $\Delta rpoS$ (blue dots). Median
271 EtBr fluorescence per cell in 10,000 SYTO-84⁺ flow cytometry events was measured every hour between 0 and 6
272 hours. Individual symbols represent the median value of EtBr fluorescence within a biological replicate. **(C)**
273 shows SL1344 $\Delta acrB$ (black diamonds) vs $\Delta acrB \Delta rpoS$ (green diamonds). Median EtBr fluorescence per cell in
274 10,000 SYTO-84⁺ flow cytometry events was measured every hour between 0 and 6 hours. Individual symbols
275 represent the median value of EtBr fluorescence within a biological replicate. Significant differences to parent
276 strain were measured by a two-way ANOVA and Sidak's multiple comparison test. At 3 hours, EtBr accumulation
277 in $\Delta acrB \Delta rpoS$ is significantly different to $\Delta acrB$ with a p value of 0.0002 (***).

278 A previous study found that increased SDS resistance in carbon-limited stationary
279 phase *E. coli* is due to decreased envelope permeability mediated by RpoS-
280 dependent and –independent mechanisms¹⁹. The role of RpoS in decreased EtBr
281 permeability in *S. Typhimurium* was therefore investigated by construction of $\Delta rpoS$
282 mutants of SL1344 and its $\Delta acrB$ variant.

283 Deletion of *rpoS* in SL1344 caused no significant difference in EtBr accumulation
284 (**Figure 5B**), although these bacteria were efflux-active so EtBr could be pumped
285 out. Comparison of the $\Delta acrB$ and $\Delta rpoS \Delta acrB$ mutants (**Figure 5C**) revealed a
286 significant difference in EtBr accumulation only around 3 h growth; the $\Delta rpoS$ mutant
287 showed a delayed decrease in EtBr accumulation, although in stationary phase the
288 two strains were similar. We conclude that in *S. Typhimurium*, although RpoS might
289 play a role in envelope remodelling, it is not essential for generation of a low-
290 permeability envelope in stationary phase, so there are likely to be RpoS-dependent
291 and –independent pathways to achieve this phenotype. Although SDS and EDTA
292 disrupt the cell envelope in different ways (detergent disruption of lipid membranes
293 versus chelation of divalent cations), it is clear that RpoS-dependent and –
294 independent mechanisms play a role in envelope remodelling in both *E. coli*¹⁹ and *S.*
295 *Typhimurium*.

296

297 **RNAseq analysis identified several pathways likely to be involved in reduced
298 envelope permeability in *S. Typhimurium***

299 Given the data above did not identify a definitive mechanism by which the stationary
300 phase cell envelope displays lower permeability to EtBr, we used RNAseq analysis
301 to identify genes and pathways that may be involved in changes to Gram-negative
302 cells as they enter stationary phase. Growing cultures of SL1344 were sampled after
303 1 hour, 3 hours and 5 hours of growth and RNA was extracted and analysed by
304 GENEWIZ Inc. Comparing SL1344 at 1 hour versus 3 or 5 hours of growth, 1228
305 (26%) and 2260 (47%) genes were differentially expressed respectively. The data is
306 deposited with Array Express (Accession: E-MTAB-9679). Differentially-expressed
307 genes were then identified that encode proteins involved in envelope remodeling in
308 stationary phase, many of which have been shown to increase barrier function
309 (Supplementary Table S1, summarized in Figure 6).

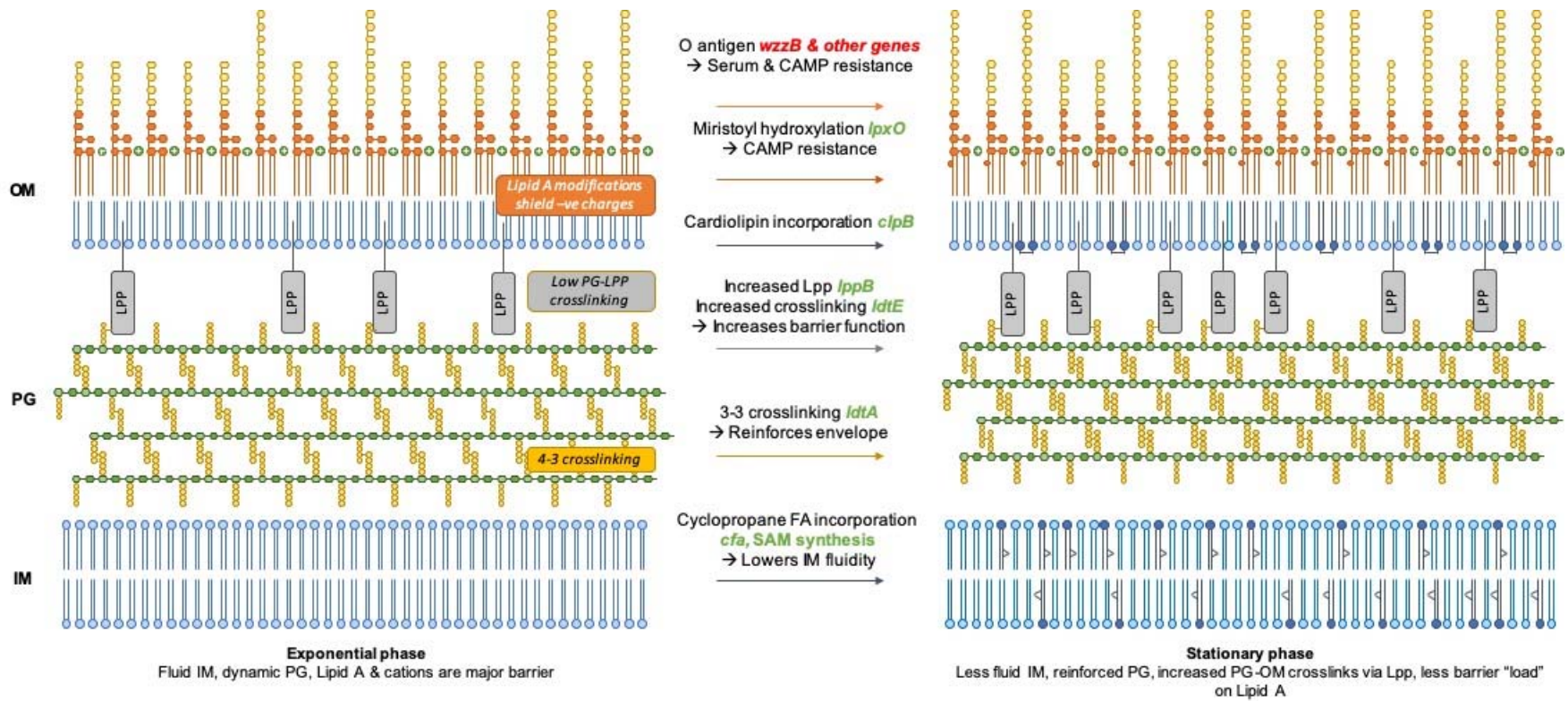
310 Previous studies have suggested that multiple layers of the cell envelope are
311 remodeled upon entry into stationary phase³⁴ and our RNASeq data support this; full
312 description of this dataset is in the supplementary material. Inner membrane fluidity
313 decreases with cyclopropane fatty acid incorporation³⁶⁻³⁸, mediated by upregulation
314 of *cfa*. Stationary phase peptidoglycan contains 3-3 (LD) rather than 4-3 (DD)
315 crosslinks^{22,39,40}; relevant transpeptidases are up- and downregulated. The quantity
316 of Lpp in the OM increases (*lppB* is upregulated) and becomes more highly
317 crosslinked to the PG (*ldtE* is upregulated²²), which has been shown to increase⁴²
318 barrier function⁴¹. OM inner leaflet cardiolipin content is known to increase⁴²
319 potentially mediated by upregulation of *clsB*. LPS modification pathways important in

320 exponential phase (e.g. the *pmr* genes which confer CAMP resistance primarily
321 through negative charge neutralization)⁴³⁻⁴⁵ are downregulated whereas *lpxO*
322 (involved in myristoyl chain hydroxylation and implicated in CAMP resistance in *K.*
323 *pneumonia*⁴⁶) is upregulated. Genes involved in O-antigen synthesis and chain
324 length regulation are downregulated; average O-antigen chain length increases in
325 stationary phase and O-antigen structure has been shown to influence serum
326 resistance⁴⁷ and CAMP susceptibility⁴⁸. Finally, genes involved in enterobacterial
327 common antigen (ECA) synthesis are downregulated; ECA is implicated in envelope
328 integrity and bile resistance.

329 Taken together, this leads to a model (Figure 6) suggesting why the exponential
330 phase cell envelope is more susceptible to attack from various factors (EtBr, CAMPs,
331 EDTA, antibiotics). Resistance to self-mediated uptake in exponential phase is
332 provided primarily by the barrier function of LPS, comprising lipid hydrophobicity and
333 crosslinking between phosphate groups and divalent cations. The LPS takes the
334 burden because the inner layers of the envelope (PG and IM) are by necessity more
335 fluid; PG is being extensively and continually remodeled to permit growth and
336 division, and the IM is similarly fluid. The reliance on the LPS as the primary barrier
337 poses problems when antimicrobials such as EDTA and CAMPs target the
338 phosphate-cation bridges. The cell responds by shielding negative charges and
339 modifying the LPS lipid content to decrease fluidity, regulated by PmrAB.

340 In stationary phase, each layer of the envelope plays a greater role in barrier function
341 because remodeling and fluidity is less of a requirement. The lipid components of the
342 IM and OM become less fluid and the PG contains more LD-crosslinks and becomes
343 more crosslinked to the OM, further strengthening the OM permeability barrier and

344 decreasing (but not eliminating) the requirement for cation crosslinking of LPS. The
345 saccharide components of the LPS provide the outermost layer of protection. This
346 “laminated” approach shares the burden of protection and generates a strong barrier
347 against multiple chemicals which seek to enter and damage the cell, reflected by the
348 increased resistance of stationary phase cells to multiple stressors.



349

350
351

Figure 6. Model showing that the differentially-expressed genes identified in the RNAseq encode proteins involved in envelope remodeling in stationary phase to increase barrier function.

352

353 **Discussion**

354 This study shows that the mechanisms that control drug accumulation are growth
355 phase dependent. In actively growing cells, efflux is fundamental to maintaining low
356 drug accumulation and subsequently survival of the bacterial population. Bacterial
357 infections are complex, and bacterial populations will often not be in a single growth
358 phase, therefore more careful consideration may be required for the most effective
359 antibiotic treatment. We have shown that stationary phase slow or non-growing cells
360 are impermeable, and that this is not due to changes in porin production but as a
361 result of membrane remodeling and increased peptidoglycan crosslinking which
362 reinforces the envelope barrier function. Treatment of chronic infections and biofilms
363 where bacterial cells are slow- or non-growing may need to be considered more
364 carefully. Successful treatment of these infections is already extremely difficult, and
365 careful consideration is already made for treatment of intrinsically impermeable
366 pathogens such as *Pseudomonas aeruginosa* and *Acinetobacter baumanii*. More
367 extensive research into the effects of an impermeable membrane on treatment
368 during infection must now be carried out.

369 Efflux pumps are only important in maintaining low drug accumulation in actively
370 growing cells which have a more permeable envelope. If an infection is actively
371 growing, it seems likely that efflux inhibitors would be effective at increasing the
372 accumulation of antibiotics within cells to potentiate their activity. However, if cells
373 are in a slow-growing or non-growing state, where membrane permeability is
374 fundamental to maintaining low drug accumulation, efflux inhibitors may not be an
375 effective treatment option. It is also possible that administering an efflux inhibitor

376 where it has no effect on treating an infection, may also lead to the development of
377 new mechanisms of AMR.

378

379 **Materials and Methods**

380 **Strains and growth conditions**

381 Unless otherwise stated, all experiments use *Salmonella enterica* serovar
382 Typhimurium (hereafter named *S. Typhimurium*⁴⁹) SL1344. The $\Delta acrB$ and $\Delta 4PAP$
383 strains ($\Delta acrA$ $\Delta acrE$ $\Delta mdsA$ $\Delta mdtA$) have been previously published^{50,51}. SL1344
384 $\Delta ompF$ and $\Delta ompC$ strains were constructed for this study using the Datsenko and
385 Wanner method of gene deletion⁵². Transcriptional reporter constructs were made by
386 fusing the promoter of each efflux pump gene to *gfp* in the pMW82 plasmid⁵³. These
387 plasmids were transformed into SL1344 and SL1344 $\Delta acrB$. *E. coli* MG1655
388 $\Delta acrB$ ¹⁵, *P. aeruginosa* PA01 $\Delta mexA$ ⁵⁴ and *K. pneumoniae* ecl8 $acrB::Gm$ ¹⁷ were
389 also used as part of this study and are previously published.

390 Unless otherwise stated, LB (Sigma) was used as growth medium for all assays.
391 One assay used MOPs minimal media (Teknova) which was supplemented with 400
392 mg/L histidine.

393 **Chromosomal insertion of *gfp* downstream of *acrB* to produce SL1344 AcrB-GFP**

395 To measure the protein level of AcrB in *S. Typhimurium*, a gene encoding a
396 monomeric super-folder GFP (msfGFP) was inserted downstream of *acrB* on the
397 chromosome to produce an AcrB-msfGFP fusion protein. This strain was created

398 using the msfGFP from the pET GFP LIC cloning vector (u-msfGFP) which was a gift
399 from Scott Gradia (Addgene plasmid # 29772 ; <http://n2t.net/addgene:29772> ;
400 RRID:Addgene_29772). Strain construction was based on the method used by
401 Bergmiller et al. (2017) in *E. coli*²⁷ where the codon optimised polylinker was used.
402 Using restriction and ligation, the *aph* gene was inserted into pET LIC vector
403 (u-msfGFP), so that strains containing the plasmid could be selected for. Using this
404 plasmid as template, *gfp* and *aph* were inserted into the chromosome downstream of
405 *acrB* in SL1344 to produce a protein fusion strain.

406

407 **Flow cytometry assay**

408 The flow cytometric EtBr accumulation assay has been previously described¹⁷. Here
409 this method was used to measure accumulation in samples from the same culture at
410 different timepoints during batch culture. Briefly, cultures were grown at 37°C
411 overnight in 5 mL of LB and sub-cultured at 4 % into fresh LB. A sample was taken
412 at 0 hours and then every hour for 6 hours during growth. At each hour, sample
413 volume was adjusted such that approximately 10⁷ cells were harvested and re-
414 suspended in 1 x Hepes Buffered Saline (5X HBS; Alfa Aesar). Cells were washed
415 and resuspended in 1 mL HBS. 100 µL of cell suspension was then further diluted
416 into 500 µL HBS and SYTOTM 84 (Thermo Fisher Scientific) and ethidium bromide
417 added to give final concentrations of 10 µM and 100 µM respectively. Samples were
418 incubated for 10 minutes before measuring accumulation by flow cytometry. Flow
419 cytometry settings and emission filters were used from Whittle et al¹⁷. Briefly, The
420 SYTO 84 fluorescence emission was collected in the YL1-H channel (585/16 nm)
421 using a 561 nm yellow laser and used to differentiate cells from acellular material.

422 EtBr fluorescence was collected using the BL3-H channel (695/40 nm) using a 488
423 nm blue laser. SYTO 84 accumulation measurements (**Figure 4**), was not a
424 repeated experiment but data was re-analysed from EtBr accumulation assays and
425 therefore fluorescence emission was collected in the YL1-H channel (585/16 nm)
426 using a 561 nm yellow laser. Nile Red accumulation was measured as previously
427 described¹⁷. In these experiments SYTO 9 (10 μ M; Thermo Fisher Scientific) was
428 used to differentiate cells from acellular particles using the BL2-H channel. Nile red
429 has an excitation of 549 nm and emission of 628 nm in the presence of
430 phospholipids, and in a neutral lipid environment (tryglycerides), the fluorescence
431 shifts to ex/em of 510/580 nm³¹. Nile red fluorescence was excited using the yellow
432 laser and detected using the YL1-H channel for orange fluorescence¹⁷.

433 **Flow cytometry assay in the presence of EDTA**

434 Growing culture samples were taken at 1, 3 and 5 hours as above. Samples were
435 made with varying concentrations of EDTA (0 μ M, 1 μ M, 10 μ M, 100 μ M, 200 μ M
436 and 500 μ M) in 500 μ L HBS. These concentrations of EDTA increased the final
437 volume of the sample because the stock concentration was limited by solubility.
438 Dyes were then added but volume added was adjusted to maintain the final
439 concentration stated above. Once the dyes were added, 100 μ L of cell suspension
440 was added and cells were incubated for 10 minutes at room temperature. Samples
441 were then analysed by flow cytometry.

442 **Whole population transcription analysis**

443 Overnight cultures containing pMW82 transcriptional reporter plasmids were diluted
444 1:10000 in MOPs minimal media, supplemented with 50 μ g/ml ampicillin. OD₆₀₀ and

445 GFP fluorescence were measured every 30 minutes for 12 hours using a Fluostar
446 Omega (BMG labtech) incubated at 37 °C. OD₆₀₀ and GFP fluorescence were
447 measured, and a minimal media only control subtracted from the data. SL1344
448 autofluorescence was removed by subtracting SL1344 fluorescence from that of
449 pMW82 strains. GFP fluorescence divided by OD₆₀₀ was used as a measurement to
450 disregard cell density across growth.

451 **Efflux assay**

452 Efflux assays were carried out as previously described as previously¹⁴. This assay
453 measures direct efflux activity of a population of cells by pre-loading cells with a
454 fluorescent efflux substrate in the presence of the proton motive force inhibitor,
455 CCCP, and re-energising cells with glucose to measure the decrease in fluorescence
456 as substrates leave the cells. Briefly, overnight cultures of SL1344 and SL1344
457 $\Delta acrB$ were sub-cultured into fresh LB and then grown for 5 hours at 37°C. At the 1,
458 3 and 5-hour time points, 10mL of culture was taken and the OD₆₀₀ measured. The
459 harvested cell pellet was then resuspended in phosphate buffer containing MgCl₂
460 buffer and each strain adjusted to the same OD₆₀₀.

461 **RNAseq**

462 The transcriptome of SL1344 and SL1344 $\Delta acrB$ were analysed at different time
463 points during growth (1, 3 and 5 hours). There were 4 replicates of each strain.
464 MOPS minimal media was inoculated at 4% with overnight cultures. Cultures were
465 incubated at 37°C, shaking for 5 hours. At 1 hour, 5 mL of culture was centrifuged at
466 3500 x g for 5 minutes at room temperature to harvest the cells. The supernatant
467 was removed and the pellet was snap frozen. At the 3 and 5- hour time points, only 1

468 mL of culture was harvested and snap frozen. GENEWIZ Inc. carried out the RNA
469 extraction, quality control, library preparation, sequencing and bioinformatic analysis.
470 Briefly, total RNA was extracted from *S. Typhimurium* cell pellets using RNeasy Plus
471 Universal kit (Qiagen), and RNA quality control was carried out using Qubit 2.0
472 Fluorometer to measure total RNA concentration and Agilent TapeStation to produce
473 an RNA integrity number (RIN) and a DV₂₀₀ score. To remove rRNA, the ribozero
474 Removal Kit was used (Illumina). The NEBNext Ultra II RNA Library Prep Kit
475 (Illumina) was used for library preparation, following the manufacturer's protocol. For
476 library preparation, cDNA was synthesised, end repaired and adenylated at the 3'
477 ends. Universal adapters were ligated to cDNA and library enrichment was carried
478 out using limited cycle PCR. Sequencing was carried out using Illumina HiSeq 4000.
479 Bioinformatic data analysis was carried out by GENEWIZ Inc. Trimmed reads were
480 mapped to the SL1344 reference genome FQ312003 using the Bowtie2 aligner.
481 Unique gene hit counts were calculated by using feature Counts from the Subread
482 package. All statistical analysis was performed using R. With the package, DESeq2,
483 a comparison of gene expression between the groups of samples was performed.
484 The Wald test was used to generate p-values and Log2 fold changes. Data is
485 accessible on ArrayExpress with the accession code E-MTAB-9679.

486

487 **Conflict of Interest Statement**

488 The authors declare that the research was conducted in the absence of any
489 commercial or financial relationships that may be considered as a conflict of interest.

490 **Authors Contributions Statement**

491 JMAB, TWO and EEW designed these assays. GFP transcriptional reporter strains
492 were constructed by ET. EEW and HM performed experiments to obtain samples for
493 RNAseq. EEW performed all other experiments. EEW analysed all data. RNAseq
494 data was analysed by EEW and TWO. This manuscript was written by EEW, JMAB,
495 TWO and MAW.

496 **Funding**

497 EEW was funded by the AAMR Wellcome Trust DTP grant 108876/B/15/Z at the
498 University of Birmingham. JMAB and HM were funded by BBSRC grant
499 BB/M02623X/1 (David Phillips Fellowship to JMAB).

500

501 **References**

- 502 1. Nikaido, H. Outer membrane barrier as a mechanism of antimicrobial
503 resistance. *Antimicrobial Agents and Chemotherapy* (1989)
504 doi:10.1128/AAC.33.11.1831.
- 505 2. Pratt, L. A., Hsing, W., Gibson, K. E. & Silhavy, T. J. From acids to *osmZ*:
506 Multiple factors influence synthesis of the OmpF and OmpC porins in
507 *Escherichia coli*. *Molecular Microbiology* (1996) doi:10.1111/j.1365-
508 2958.1996.tb02532.x.
- 509 3. Dupont, H. *et al.* Structural alteration of OmpR as a source of ertapenem
510 resistance in a CTX-M-15-producing *Escherichia coli* O25b:H4 sequence type
511 131 clinical isolate. *Antimicrob. Agents Chemother.* (2017)
512 doi:10.1128/AAC.00014-17.

513 4. Dé, E. *et al.* A new mechanism of antibiotic resistance in Enterobacteriaceae
514 induced by a structural modification of the major porin. *Mol. Microbiol.* (2001)
515 doi:10.1046/j.1365-2958.2001.02501.x.

516 5. Bajaj, H. *et al.* Molecular Basis of filtering carbapenems by porins from
517 β lactam-resistant clinical strains of *Escherichia coli*. *J. Biol. Chem.* (2016)
518 doi:10.1074/jbc.M115.690156.

519 6. Hancock, R. E. W. & Bell, A. Antibiotic uptake into gram-negative bacteria. in
520 *Current Topics in Infectious Diseases and Clinical Microbiology* (1989).
521 doi:10.1007/978-3-322-86064-4_5.

522 7. Hancock, R. E. W., Raffle, V. J. & Nicas, T. I. Involvement of the outer
523 membrane in gentamicin and streptomycin uptake and killing in *Pseudomonas*
524 *aeruginosa*. *Antimicrob. Agents Chemother.* (1981) doi:10.1128/AAC.19.5.777.

525 8. Delcour, A. H. Outer membrane permeability and antibiotic resistance.
526 *Biochimica et Biophysica Acta - Proteins and Proteomics* (2009)
527 doi:10.1016/j.bbapap.2008.11.005.

528 9. Hancock, R. E. Alterations in outer membrane permeability. *Annual review of*
529 *microbiology* (1984) doi:10.1146/annurev.mi.38.100184.001321.

530 10. Hassan, K. A. *et al.* Pacing across the membrane: the novel PACE family of
531 efflux pumps is widespread in Gram-negative pathogens. *Res. Microbiol.*
532 (2018) doi:10.1016/j.resmic.2018.01.001.

533 11. Blair, J. M. A. *et al.* Expression of homologous RND efflux pump genes is
534 dependent upon AcrB expression: Implications for efflux and virulence inhibitor

535 design. *J. Antimicrob. Chemother.* (2015) doi:10.1093/jac/dku380.

536 12. Webber, M. A. & Piddock, L. J. V. Absence of mutations in *marRAB* or *soxRS*
537 in *acrB*-overexpressing fluoroquinolone-resistant clinical and veterinary
538 isolates of *Escherichia coli*. *Antimicrob. Agents Chemother.* (2001)
539 doi:10.1128/AAC.45.5.1550-1552.2001.

540 13. Chowdhury, N. et al. Identification of AcrAB-TolC Efflux Pump Genes and
541 Detection of Mutation in Efflux Repressor AcrR from Omeprazole Responsive
542 Multidrug-Resistant *Escherichia coli* Isolates Causing Urinary Tract Infections.
543 *Microbiol. Insights* (2019) doi:10.1177/1178636119889629.

544 14. Smith, H. E. & Blair, J. M. A. Redundancy in the periplasmic adaptor proteins
545 AcrA and AcrE provides resilience and an ability to export substrates of
546 multidrug efflux. *J. Antimicrob. Chemother.* (2014) doi:10.1093/jac/dkt481.

547 15. Wang-Kan, X. et al. Lack of AcrB efflux function confers loss of virulence on
548 *Salmonella enterica* serovar typhimurium. *MBio* (2017)
549 doi:10.1128/mBio.00968-17.

550 16. Blair, J. M. A. & Piddock, L. J. V. How to measure export via bacterial
551 multidrug resistance efflux pumps. *MBio* (2016) doi:10.1128/mBio.00840-16.

552 17. Whittle, E. E. et al. Flow Cytometric Analysis of Efflux by Dye Accumulation.
553 *Front. Microbiol.* (2019) doi:10.3389/fmicb.2019.02319.

554 18. Bailey, A. M., Webber, M. A. & Piddock, L. J. V. Medium plays a role in
555 determining expression of *acrB*, *marA*, and *soxS* in *Escherichia coli*.
556 *Antimicrob. Agents Chemother.* (2006) doi:10.1128/AAC.50.3.1071-

557 1074.2006.

558 19. Mitchell, A. M., Wang, W. & Silhavy, T. J. Novel RpoS-dependent mechanisms
559 strengthen the envelope permeability barrier during stationary phase. *J.*
560 *Bacteriol.* (2017) doi:10.1128/JB.00708-16.

561 20. Allen, R. J. & Scott, G. K. Biosynthesis and turnover of outer-membrane
562 proteins in *Escherichia coli* ML308-225. *Biochem. J.* **182**, 407–412 (1979).

563 21. WENSINK, J., GILDEN, N. & WITHOLT, B. Attachment of Lipoprotein to the
564 Murein of *Escherichia coli*. *Eur. J. Biochem.* (1982) doi:10.1111/j.1432-
565 1033.1982.tb06479.x.

566 22. Glauner, B., Holtje, J. V. & Schwarz, U. The composition of the murein of
567 *Escherichia coli*. *J. Biol. Chem.* (1988) doi:10.1016/s0021-9258(19)81481-3.

568 23. El-Khani, M. A. & Stretton, R. J. Effect of growth medium on the lipid
569 composition of log and stationary phase cultures of *Salmonella typhimurium*.
570 *Microbios* (1981).

571 24. Grogan, D. W. & Cronan, J. E. Cyclopropane ring formation in membrane
572 lipids of bacteria. *Microbiol. Mol. Biol. Rev.* (1997) doi:10.1128/61.4.429-
573 441.1997.

574 25. Mengin-Lecreulx, D. & Van Heijenoort, J. Effect of growth conditions on
575 peptidoglycan content and cytoplasmic steps of its biosynthesis in *Escherichia*
576 *coli*. *J. Bacteriol.* (1985) doi:10.1128/jb.163.1.208-212.1985.

577 26. Chai, Q., Webb, S. R., Wang, Z., Dutch, R. E. & Wei, Y. Study of the
578 degradation of a multidrug transporter using a non-radioactive pulse chase

579 method. *Anal. Bioanal. Chem.* (2016) doi:10.1007/s00216-016-9871-7.

580 27. Bergmiller, T. *et al.* Biased partitioning of the multidrug efflux pump AcrAB-
581 TolC underlies long-lived phenotypic heterogeneity. *Science* (80-.). (2017)
582 doi:10.1126/science.aaf4762.

583 28. Pagès, J. M. & Amaral, L. Mechanisms of drug efflux and strategies to combat
584 them: Challenging the efflux pump of Gram-negative bacteria. *Biochimica et
585 Biophysica Acta - Proteins and Proteomics* (2009)
586 doi:10.1016/j.bbapap.2008.12.011.

587 29. Pagès, J. M., Masi, M. & Barbe, J. Inhibitors of efflux pumps in Gram-negative
588 bacteria. *Trends in Molecular Medicine* (2005)
589 doi:10.1016/j.molmed.2005.06.006.

590 30. Nikaido, H. Small Things Considered: The Limitations of LB Medium. *Small
591 Things Considered* (2009).

592 31. Greenspan, P. & Fowler, S. D. Spectrofluorometric studies of the lipid probe,
593 nile red. *J. Lipid Res.* (1985) doi:10.1016/S0022-2275(20)34307-8.

594 32. Murata, T., Tseng, W., Guina, T., Miller, S. I. & Nikaido, H. PhoPQ-mediated
595 regulation produces a more robust permeability barrier in the outer membrane
596 of *Salmonella enterica* serovar typhimurium. *J. Bacteriol.* **189**, (2007).

597 33. Leive, L. Release of lipopolysaccharide by EDTA treatment of *E. coli*.
598 *Biochem. Biophys. Res. Commun.* (1965) doi:10.1016/0006-291X(65)90191-9.

599 34. McLeod, G. I. & Spector, M. P. Starvation- and stationary-phase-induced
600 resistance to the antimicrobial peptide polymyxin B in *Salmonella typhimurium*

601 is RpoS (σ (S)) independent and occurs through both *phoP*-dependent and -
602 independent pathways. *J. Bacteriol.* **178**, (1996).

603 35. Agrawal, A., Rangarajan, N. & Weisshaar, J. C. Resistance of early stationary
604 phase *E. coli* to membrane permeabilization by the antimicrobial peptide
605 Cecropin A. *Biochim. Biophys. Acta - Biomembr.* **1861**, (2019).

606 36. Bianco, C. M., Fröhlich, K. S. A. & Vanderpool, C. K. Bacterial cyclopropane
607 fatty acid synthase mRNA is targeted by activating and repressing small
608 RNAs. *J. Bacteriol.* (2019) doi:10.1128/JB.00461-19.

609 37. Qi, Y., Liu, H., Chen, X. & Liu, L. Engineering microbial membranes to
610 increase stress tolerance of industrial strains. *Metabolic Engineering* (2019)
611 doi:10.1016/j.ymben.2018.12.010.

612 38. Huisman, G. W., Siegele, D. a, Zambrano, M. M. & Kolter, R. Morphological
613 and physiological changes during stationary phase. *Escherichia coli*
614 *Salmonella Cell. Mol. Biol.* (1996).

615 39. Morè, N. *et al.* Peptidoglycan remodeling enables *Escherichia coli* to survive
616 severe outer membrane assembly defect. *MBio* (2019)
617 doi:10.1128/mBio.02729-18.

618 40. Magnet, S., Dubost, L., Marie, A., Arthur, M. & Gutmann, L. Identification of the
619 L,D-transpeptidases for peptidoglycan cross-linking in *Escherichia coli*. *J.*
620 *Bacteriol.* **190**, (2008).

621 41. Peters, K. *et al.* Copper inhibits peptidoglycan LD-transpeptidases suppressing
622 β -lactam resistance due to bypass of penicillin-binding proteins. *Proc. Natl.*

623 *Acad. Sci. U. S. A.* (2018) doi:10.1073/pnas.1809285115.

624 42. Hiraoka, S., Matsuzaki, H. & Shibuya, I. Active increase in cardiolipin synthesis
625 in the stationary growth phase and its physiological significance in *Escherichia*
626 *coli*. *FEBS Lett.* **336**, (1993).

627 43. Raetz, C. R. H., Reynolds, C. M., Trent, M. S. & Bishop, R. E. Lipid a
628 modification systems in gram-negative bacteria. *Annual Review of*
629 *Biochemistry* (2007) doi:10.1146/annurev.biochem.76.010307.145803.

630 44. May, J. F. & Groisman, E. A. Conflicting roles for a cell surface modification in
631 *Salmonella*. *Mol. Microbiol.* **88**, (2013).

632 45. Agrawal, A. & Weisshaar, J. C. Effects of alterations of the *E. coli*
633 lipopolysaccharide layer on membrane permeabilization events induced by
634 Cecropin A. *Biochim. Biophys. Acta - Biomembr.* **1860**, (2018).

635 46. Llobet, E. et al. Deciphering tissue-induced *Klebsiella pneumoniae* lipid a
636 structure. *Proc. Natl. Acad. Sci. U. S. A.* (2015) doi:10.1073/pnas.1508820112.

637 47. Bravo, D. et al. Growth-phase regulation of lipopolysaccharide O-antigen chain
638 length influences serum resistance in serovars of *Salmonella*. *J. Med.*
639 *Microbiol.* **57**, (2008).

640 48. Ricci, V., Zhang, D., Teale, C. & Piddock, L. J. V. The o-antigen epitope
641 governs susceptibility to colistin in *Salmonella enterica*. *MBio* **11**, (2020).

642 49. Brenner, F. W., Villar, R. G., Angulo, F. J., Tauxe, R. & Swaminathan, B.
643 *Salmonella* nomenclature. *Journal of Clinical Microbiology* (2000)
644 doi:10.1128/jcm.38.7.2465-2467.2000.

645 50. Eaves, D. J., Ricci, V. & Piddock, L. J. V. Expression of *acrB*, *acrF*, *acrD*,
646 *marA*, and *soxS* in *Salmonella enterica* Serovar Typhimurium: Role in Multiple
647 Antibiotic Resistance. *Antimicrob. Agents Chemother.* (2004)
648 doi:10.1128/AAC.48.4.1145-1150.2004.

649 51. McNeil, H. E. *et al.* Identification of binding residues between periplasmic
650 adapter protein (PAP) and RND efflux pumps explains PAP-pump promiscuity
651 and roles in antimicrobial resistance. *PLoS Pathog.* (2019)
652 doi:10.1371/JOURNAL.PPAT.1008101.

653 52. Datsenko, K. A. & Wanner, B. L. One-step inactivation of chromosomal genes
654 in *Escherichia coli* K-12 using PCR products. *Proc. Natl. Acad. Sci. U. S. A.*
655 (2000) doi:10.1073/pnas.120163297.

656 53. Bumann, D. & Valdivia, R. H. Identification of host-induced pathogen genes by
657 differential fluorescence induction reporter systems. *Nat. Protoc.* (2007)
658 doi:10.1038/nprot.2007.78.

659 54. Held, K., Ramage, E., Jacobs, M., Gallagher, L. & Manoil, C. Sequence-
660 verified two-allele transposon mutant library for *Pseudomonas aeruginosa*
661 PAO1. *J. Bacteriol.* (2012) doi:10.1128/JB.01479-12.

662